Transient electronic and magnetic structures of nickel heated by ultrafast laser pulses

T. Kachel,[1] N. Pontius,[1] C. Stamm,[1] M. Wietstruk,[1] E. F. Aziz,[1] H. A. Dürr,[1] W. Eberhardt,[1] and F. M. F. de Groot[2]
[1]*Helmholtz-Zentrum Berlin für Materialien und Energie GmbH, BESSY II, Albert-Einstein-Str. 15, 12489 Berlin, Germany*
[2]*Department of Inorganic Chemistry and Catalysis, Utrecht University, Sorbonnelaan 16, 3584 CA Utrecht, The Netherlands*
(Received 20 February 2009; revised manuscript received 14 July 2009; published 11 September 2009)

We investigate the evolution of the Ni electronic and magnetic structure on fs to ps time scales following fs-laser excitation. Within 200 fs after excitation the Ni $3d$ ferromagnetic moment is reduced as probed by x-ray magnetic circular dichroism. At the same time the Ni $3d$ electronic structure undergoes pronounced changes as demonstrated by x-ray absorption spectroscopy. We show that the latter persists also into thermal equilibrium which is reached on the ps time scale. Cluster calculations identify a reduction in $3d-4sp$ hybridization possibly associated with phonon-driven spin-flip excitations.

DOI: 10.1103/PhysRevB.80.092404 PACS number(s): 75.70.−i, 71.20.Be, 78.47.J−

The microscopic understanding of finite-temperature itinerant magnetism remains elusive in spite of many decades of experimental and theoretical investigations.[1] Ferromagnetic Ni is a prime example: the strong on-site electron correlations of the Ni $3d$ shell are responsible for local magnetic moments. However, there is also significant hybridization of $3d$ levels especially with the more itinerant $4sp$ states of neighboring atoms. This causes a challenging interplay between magnetic properties of localized and itinerant valence electrons.

Two main models exist for describing the decrease in the magnetization at finite temperatures. In the first, collective spin-wave excitations (magnons) are commonly associated with the quenching of long-range ferromagnetic order with increasing temperature.[2,3] They are observed in Ni by inelastic neutron scattering[4,5] and above T_C result in paramagnetic spin fluctuations[6] of local magnetic momenta.[7] The second model is used especially when approaching T_C, where the reduced size of the magnetic moments demonstrates the importance of electronic spin-flip excitations in Ni.[8] For instance, in Stoner excitations, an electron is excited from an occupied state of the majority-spin band to an empty state of the minority-spin band, thus probing the average exchange splitting of the Ni $3d$ levels.[9] Similarly, Elliott-Yafet-type spin-flip scattering of electrons at phonons are believed to promote ultrafast demagnetization following optical fs-laser heating.[10,11] We have recently shown, using time-resolved fs x-ray absorption spectroscopy (XAS) and x-ray magnetic circular dichroism (XMCD) that changes in spin angular momentum associated with spin-flip excitations are compensated by the lattice on a time scale of 120 fs.[12] The question arises now whether also in thermal equilibrium such ultrafast transfer of angular momentum between the spin and lattice subsystems is possible and indeed may be required for angular-momentum conservation across the magnetic phase transition.[13]

In this Brief Report, we compare the electronic state of a thin Ni film 200 fs after excitation with a fs-laser pulse, to the same film after 50–100 ps, i.e., in thermal equilibrium but at elevated temperature. By heating with an ultrafast laser pulse in our pump-probe setup,[12] we are able to acquire temperature-induced changes in the Ni L_3-edge XAS and XMCD measurements with unprecedented accuracy. With increasing temperature, the Ni XAS line shape exhibits pronounced changes, while the Ni XMCD simply rescales proportional to the vanishing long-range ferromagnetic order upon approaching T_C. By comparing the measurements to cluster calculations, we demonstrate that in Ni the nearest-neighbor $3d-4sp$ hybridization is reduced at high temperatures. We interpret the change in the Ni electronic structure as being caused by incoherent spin-flip excitations.

The experiments were performed at the BESSY II beamline UE56/1-PGM, which is optimized for infrared laser pump—soft x-ray probe experiments.[12] Circularly polarized x-rays were transmitted through the thin-film sample to measure XAS and XMCD spectra, i.e., the average and the difference in x-ray absorption while the sample magnetization is reversed in an applied magnetic field. The sample consisted of a $\approx$35 nm Ni film evaporated *in situ* under ultrahigh vacuum conditions onto a 500-nm-thick Al foil of 5×5 mm^2 lateral size. This resulted in an uncontaminated, homogeneous, polycrystalline film which is magnetically saturated in the film plane by the applied magnetic field as checked with static XMCD measurements. A key feature of the present experiment is that the sample temperature is changed by heating with a fs-laser pulse (50 fs pulse duration, 780 nm wavelength, 3 kHz repetition rate, fluence up to 15 mJ/cm^2). The pump-laser spot size on the sample was 1.5×0.5 mm^2, larger than the x-ray probe size (1.0×0.2 mm^2). The synchrotron repetition rate is much higher than that of the fs laser, thus electronic gating allowed us to simultaneously record spectra of the sample just after laser heating and of the cool sample in between two laser pulses. As the time between these two measurements is just 167 μs, we achieved a much higher accuracy for determining temperature-dependent changes in the XAS and XMCD spectra than by conventional variations in the sample temperature.

In Fig. 1 we show the spectral and temporal response of a 35 nm Ni film at the L_3 absorption edge. Excitation of the sample by a fs-laser pulse results in a shift of the absorption edge toward lower photon energy, see Fig. 1(a). The difference in the excited spectrum and the spectrum in equilibrium is plotted as circles in Fig. 1(b). The temporal response of this transient line shift is taking place on the fs time range, associated with the dynamics of hot electrons populating previously unoccupied states near the Fermi level.[14] Relaxation to an intermediate level sets in with a time constant of 500 fs,

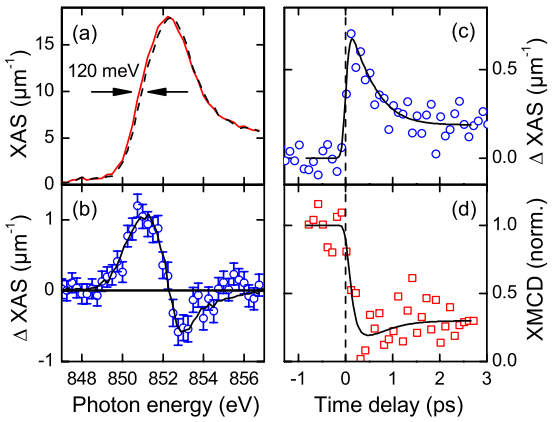

FIG. 1. (Color online) (a) L_3 absorption edge of a 35 nm Ni film measured with fs x-ray pulses, 200 fs after laser excitation (red line) and in equilibrium, i.e., before laser excitation (dashed line). Their difference is plotted as circles in (b), together with the difference after 50 ps (line, multiplied by 4). (c) circles denote the change of XAS intensity vs pump-probe time delay, with photon energy set to 851 eV, the maximum difference found in (b). In (a)–(c), linearly polarized x-rays with perpendicular incidence were used. (d) XMCD at the L_3 edge normalized to nonpumped signal, measured with circularly polarized x-rays, 60° angle between sample surface and x-ray propagation direction, and applied field of ± 0.24 T (squares). Solid lines in (c) and (d) are fits according to a three-temperature model. The pump-laser fluence was 8 mJ/cm^2.

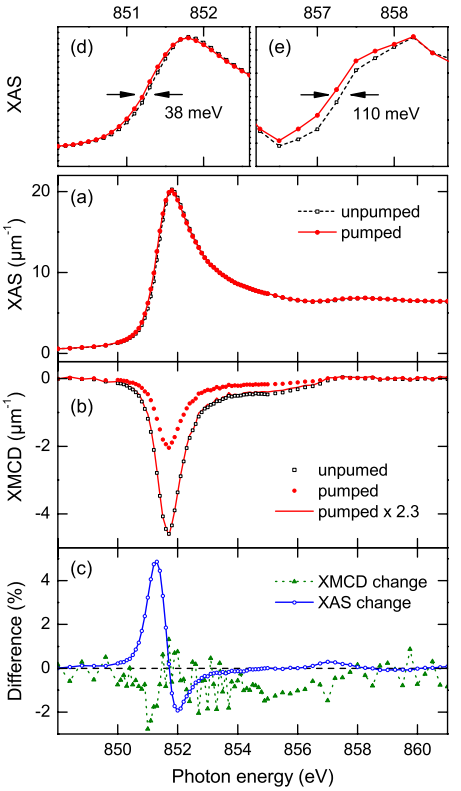

FIG. 2. (Color online) Ni L_3 (a) XAS and (b) XMCD spectra for a 30 nm Ni film at room temperature (0.46 T_C, open squares) and temperature of 0.93 T_C (solid circles). The line in (b) indicates the high-temperature XMCD spectrum multiplied by 2.3. (c) Difference curves for XAS (open circles) and XMCD (solid triangles). Enlarged view of the data in (a): leading XAS edge (d) and XAS satellite (e).

as is apparent from the temporal evolution shown in Fig. 1(c). The spin system, investigated here by a measurement of the XMCD at the L_3 edge, also reacts on a comparable time scale. The drop of the dichroic signal at time zero, as shown in Fig. 1(d), reflects the laser-induced demagnetization of ferromagnetic Ni. These measurements were acquired in the femtoslicing mode with a temporal resolution of 100 fs, yielding similar results as our previous experiments with a 15 nm film.[12] However the goal of this paper is to further investigate the spectral signature of laser-heated nickel with high-resolution x-ray spectroscopy. To achieve this we now work with the natural pulse length of the synchrotron source ($\approx$50 ps) and select a delay of 50 ps between laser pump and x-ray probe. This guarantees that the electronic, spin and lattice excitations of the Ni film are in thermal equilibrium[14] corresponding to an elevated temperature. Comparing the spectra measured after 200 fs and 50 ps, we find that the laser-induced XAS line shift is similar but smaller when measured 50 ps after pumping. If scaled by a factor of 4, the XAS change, plotted as a line in Fig. 1(b), perfectly follows the data as measured for a delay time of 200 fs (circles). This striking qualitative agreement is a strong indication that the observed line-shift scales with the electronic temperature in the Ni film.

In Fig. 2 we compare (a) XAS and (b) XMCD spectra of a Ni film at room temperature to the corresponding spectra at elevated temperature, 100 ps after heating with a laser pulse. The most pronounced temperature effect is the reduction in the XMCD intensity by a factor of 2.3, as plotted in Fig. 2(b). From this reduction in the magnetic moment a sample temperature of T/T_C=0.93 can be estimated.[15] Additional, more subtle temperature-dependent changes become apparent when comparing the difference XAS and XMCD spectra for the two temperatures in Fig. 2(c). The derivativelike lineshape of the XAS difference indicates a shift of the leading L_3 edge of the main absorption peak to lower photon energy with increasing temperature. This energy shift amounts to -38 ± 5 meV as shown in Fig. 2(d). We observed that this shift roughly scales linearly with the pump-laser fluence, i.e., sample temperature (not shown). For the Ni L_3 satellite we find an even stronger temperature effect: the leading satellite edge shifts by -110 ± 20 meV [Fig. 2(e)]. In contrast, the difference between the two XMCD spectra [with the high-temperature curve scaled to the room-temperature spectrum, see Fig. 2(c)] shows no derivativelike lineshape comparable to the XAS. This demonstrates that in Ni any temperature-dependent energy shift is significantly smaller for the XMCD than for the XAS spectra. While the shift of the XAS main peak resembles that observed on the 120 fs time scale,[12] the even larger shift of the XAS satellite and the absence of comparable shifts in the XMCD are new observations. The identification of all three effects in equilibrium conditions at elevated temperatures represents the central result of this paper. In order to elucidate their microscopic origin, we will now model the temperature-dependent behavior of the XAS and XMCD line shape in a cluster-model calculation.

Calculations of Ni XAS and XMCD spectra have been

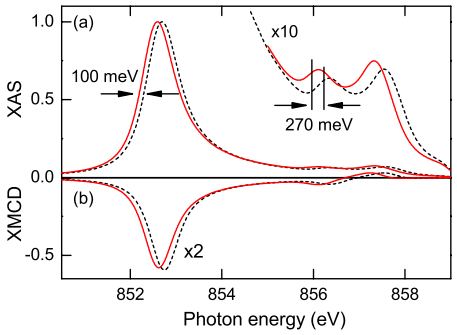

FIG. 3. (Color online) Cluster calculations of Ni L_3 (a) XAS and (b) XMCD spectra comparing the low-temperature state (black dashed lines) to states (red lines) with V reduced by 5%.

reported using two complementary approaches, based on either *ab initio* bandstructure[16–18] or with the inclusion of $2p3d$ multiplet interactions.[19–21] Of crucial importance is a realistic modeling of the XAS and XMCD satellite structures which are not visible for the more itinerant $3d$ transition metals Co and Fe.[22] While the band-structure approach fails to reproduce the XMCD satellite,[16–18] it assigns the XAS satellite to a critical point in the Ni bandstructure.[16,17] However, this can only be achieved by renormalizing electronic (exchange and spin-orbit) interaction parameters for the final state containing a core hole. This mimics many particle interactions which are neglected in a single-electron approximation.[16,17] We, therefore, used the second approach based on an Anderson impurity picture where electron-electron interactions are taken into account at a Ni central atom for ground and core-hole final states. The salient features of the Ni XAS and XMCD spectra can be reproduced by a cluster model with a ground state consisting of $3d^8\upsilon^2$, $3d^9\upsilon^1$, and $3d^{10}$ configurations.[19] In addition to Ref. 19, we approximated the Ni band structure by hopping of Ni $3d$ electrons to neighboring valence orbitals, υ, of mainly $4sp$ character by introducing a bandwidth to the $3d^9\upsilon^1$ state, thus, reproducing the experimentally observed asymmetry of the XAS/XMCD main peak.[23] In the x-ray absorption process transitions from this state to the $2\underline{p}3d^{10}\upsilon^1$ final states (here $2\underline{p}$ denotes a core hole) give the dominant contribution to the XAS and XMCD main peaks. Transitions into the $2\underline{p}3d^9\upsilon^2$ final states mainly give rise to the satellite feature in XAS and XMCD.[19] The energy difference in $2\underline{p}3d^9\upsilon^2$ and $2\underline{p}3d^{10}\upsilon^1$ basis states is $\Delta+U-Q$ (see Ref. 23). Due to mixing of these configurations, their energy separation is also influenced by the $3d-4sp$ hybridization V.

Figure 3 illustrates the results of the cluster calculations for the ground state and the high-temperature state, which was modeled by modified electron-interaction parameters. We find that reducing the nearest-neighbor $3d-4sp$ hybridization V gives the best accordance with our experimental observation, an energy shift of the XAS satellite that is significantly larger than that of the main absorption line [Fig. 3(a)]. Only negligible peak shifts are generated by a reduction in the magnetic exchange coupling to zero (expected for the paramagnetic phase) and by a 5% variation in the crystal field (both not shown). The spectra were also found to be insensitive to a Boltzmann-type population of excited states even up to electron temperatures of 1500 K. It is conceivable that a more realistic model of the Ni band structure could cause the main XAS line to shift due to a temperature-dependent smearing of the electronic population near the Fermi level. Recent *ab initio* calculations of XAS and XMCD spectra, looking at laser-induced repopulation and electron thermalization, indeed reproduce the shift of the main L_3 absorption line.[24] However, any change in the electron population is unlikely to explain the much larger energy shift observed for the Ni XAS satellite which clearly points to an electron-correlation-induced effect. The calculated shifts [Fig. 3(a)] of the XAS main peak and satellite of 100 and 270 meV, respectively, correspond to conditions reached only during a few 100 fs (Fig. 1), while the shifts in Fig. 2 can be reproduced by a change in V by -2%. While we cannot rule out that also U and Q display a certain temperature dependence, the reduction in V with increasing temperature is dominant. Thus the spectra demonstrate without doubt that the coupling between $3d$ and $4sp$ decreases with increasing temperature. The consequence is a narrowing of the $3d$ band while the $4sp$ states remain itinerant.

A further implication of our cluster calculations is that similar shifts as in XAS should be visible in the XMCD spectra as well. Figure 3(b) shows the XMCD spectra calculated for reducing V as for Fig. 3(a). This indicates that if the electronic structure of a Ni atom as probed by XAS is modified, the XMCD spectrum displaying the magnetic response is affected similarly. Surprisingly these XMCD shifts are not observed experimentally [see Fig. 2(c)]. We can therefore conclude that atoms exhibiting XAS shifts do not contribute to the long-range magnetic ordering as measured by XMCD.[25] The number of photons from one laser pulse corresponds to only $\approx 2-3\%$ of the Ni atoms in the irradiated volume of the sample. This is much less than the reduction in magnetic ordering (down to 44% of its initial value), a process that is very efficient due to the collective nature of the exchange interaction.

Now we discuss the resemblance of our observations in thermal equilibrium (Fig. 2) with those on the femtosecond time scale (Fig. 1). We argued in Ref. 12 that during fs-laser excitation hot electrons are causing decoherence of the $3d$ wave function, which is reflected in reduced $3d-4sp$ hybridization matrix elements. This process is accompanied by a novel fs spin-lattice relaxation mechanism, i.e., a coupling of spin-flip excitations to phonons.[10] A recent *ab initio* calculation shows that such an Elliott-Yafet mechanism indeed is able to facilitate ultrafast transfer of angular momentum to the lattice.[11] The much higher excitation in the fs regime results in up to four times larger XAS peak shifts compared to the equilibrium conditions below T_C [see Fig. 1(b)]. The fs excitation corresponds to electron temperatures well above 1000 K,[14] which in thermal equilibrium would only be reached far in the paramagnetic phase. Our results from Fig. 2 demonstrate that also at moderately increased temperature, phonons are most likely responsible for the $3d-4sp$ hybridization decrease. The absence of ferromagnetic order in the XAS shift points toward the presence of spin-flip excitations in such phonon-induced processes. In Ni the atomic magnetic moment is close to 0.5 μ_B. One spin-flip process

reduces the magnetic moment by 2 μ_B, therefore compensating the ferromagnetic moments of four Ni atoms. Although we do not directly measure the lifetime of such spin-flip excitations, the comparison to the fs processes in Fig. 1 suggests similar (fs) time scales in thermal equilibrium. Within this framework, thermal equilibrium is described as a delicate balance of spin excitations that do both create and annihilate ferromagnetic order.

In conclusion, we find that at elevated temperature the electronic structure of Ni is characterized by a shift of the L_3 absorption line to lower photon energies and an even larger shift of the L_3 satellite. Cluster calculations explain this by a reduction in the nearest-neighbor $3d-4sp$ hybridization. In contrast, the experimental L_3 dichroic signal does not shift. This indicates that Ni atoms responsible for the line shift do not carry ferromagnetic order. Thus they can be associated with short-lived spin-flip excitations, leading to a spin-lattice relaxation during their lifetime. Our results show that similar phenomena as found for fs-laser excitation[12] also occur in thermal equilibrium, paving the way for a theoretical description of these effects.

We thank T. Quast, R. Mitzner, K. Holldack, D. Ponwitz, and S. Khan for their help during the measurements, and P. Oppeneer for stimulating discussions. This work was supported by the European Union.

[1] *Band-Ferromagnetism: Ground State and Finite-Temperature Phenomena*, Lecture Notes in Physics, edited by W. N. K. Baberschke and M. Donath (Springer, Berlin, 2001).
[2] S. V. Halilov, A. Y. Perlov, P. M. Oppeneer, and H. Eschrig, Europhys. Lett. **39**, 91 (1997).
[3] M. Pajda, J. Kudrnovský, I. Turek, V. Drchal, and P. Bruno, Phys. Rev. B **64**, 174402 (2001).
[4] H. A. Mook, J. W. Lynn, and R. M. Nicklow, Phys. Rev. Lett. **30**, 556 (1973).
[5] J. W. Lynn and H. A. Mook, Phys. Rev. B **23**, 198 (1981).
[6] Y. J. Uemura, G. Shirane, O. Steinsvoll, and J. Wicksted, Phys. Rev. Lett. **51**, 2322 (1983).
[7] M. Acet, E. F. Wassermann, K. Andersen, A. Murani, and O. Schärpff, Europhys. Lett. **40**, 93 (1997).
[8] A. V. Ruban, S. Khmelevskyi, P. Mohn, and B. Johansson, Phys. Rev. B **75**, 054402 (2007).
[9] J. Kirschner and E. Langenbach, Solid State Commun. **66**, 761 (1988).
[10] B. Koopmans, J. J. M. Ruigrok, F. Dalla Longa, and W. J. M. de Jonge, Phys. Rev. Lett. **95**, 267207 (2005).
[11] D. Steiauf and M. Fähnle, Phys. Rev. B **79**, 140401(R) (2009).
[12] C. Stamm *et al.*, Nature Mater. **6**, 740 (2007).
[13] A. Einstein and W. J. de Haas, Verhandl. DPG **17**, 152 (1915).
[14] H.-S. Rhie, H. A. Dürr, and W. Eberhardt, Phys. Rev. Lett. **90**, 247201 (2003).
[15] W. von der Linden, M. Donath, and V. Dose, Phys. Rev. Lett. **71**, 899 (1993).
[16] C. T. Chen, N. V. Smith, and F. Sette, Phys. Rev. B **43**, 6785 (1991).
[17] N. V. Smith, C. T. Chen, F. Sette, and L. F. Mattheiss, Phys. Rev. B **46**, 1023 (1992).
[18] A. I. Nesvizhskii, A. L. Ankudinov, J. J. Rehr, and K. Baberschke, Phys. Rev. B **62**, 15295 (2000).
[19] G. van der Laan and B. T. Thole, J. Phys.: Condens. Matter **4**, 4181 (1992).
[20] A. Tanaka and T. Jo, J. Phys. Soc. Jpn. **61**, 2669 (1992).
[21] F. M. F. de Groot, J. Electron Spectrosc. Relat. Phenom. **67**, 529 (1994).
[22] C. T. Chen, Y. U. Idzerda, H.-J. Lin, N. V. Smith, G. Meigs, E. Chaban, G. H. Ho, E. Pellegrin, and F. Sette, Phys. Rev. Lett. **75**, 152 (1995).
[23] Low-temperature Ni spectra were calculated with a $3d-4sp$ hybridization $V=1.8$ eV, a $3d$ Coulomb interaction $U=2.5$ eV and a $2p-3d$ Coulomb interaction $Q=3.7$ eV. A 3 eV bandwidth for the $3d^9v^1$ states was modeled by nine equidistant states with values of the $3d-4sp$ charge-transfer energy, Δ, ranging from -1.5 to 1.5 eV. C_{4h} symmetry and a 1 eV crystal field resulted in a ground state with 15% $3d^8v^2$, 51% $3d^9v^1$, and 34% $3d^{10}$ weights. Final state core-hole lifetime and experimental energy resolution were taken into account by Lorentian and Gaussian broadenings of 0.3 and 0.15 eV FWHM, respectively.
[24] K. Carva, D. Legut, and P. M. Oppeneer, Europhys. Lett. **86**, 57002 (2009).
[25] Note that the cluster calculations predict local magnetic moments whereas the experiment measures their value averaged over the probe volume.